Crystal chemistry of alkali-deficient schorl and tourmaline structural relationships

FRANKLIN F. FOIT, JR.

Department of Geology, Washington State University, Pullman, Washington 99164, U.S.A.

ABSTRACT

The structure of an aluminous, alkali-deficient schorl has been refined ($R = 0.054$ for 3084 intensity data) and its data integrated with those of 12 other refined tourmaline structures to provide a better understanding of the structural accommodation of diverse substitutions in the tourmaline group. Alkali-deficient schorl, $(Na_{0.55}\square_{0.45})(Fe^{2+}_{1.76}Al_{0.89}Mg_{0.33}Ti_{0.02})Al_6(BO_3)_3(Si_{5.86}Al_{0.14})O_{18.48}((OH)_{3.38}F_{0.14})$, is rhombohedral with $a = 15.963(3)$ and $c = 7.148(2)$ Å; its space group is $R3m$.

The 3a alkali site in the alkali-deficient schorl with an occupancy of $(Na_{0.55}\square_{0.45})$ is the largest yet observed in tourmaline. Substitution of cations smaller than Na, notably Ca, affects the configuration of the six-membered tetrahedral ring by decreasing its degree of "crimping" and by increasing its ditrigonality and the distortion of its tetrahedra. The only observed effect of Al → Si substitution is an increase in the size of the tetrahedra. $R^{2+} \rightarrow R^{3+}$ substitution in the 9b octahedral site in response to the dehydroxylation-type substitution, $(OH)^- + R^{2+} = O^{2-} + R^{3+}$, and alkali defect-type substitution, $R^+ + R^{2+} = {}^{3a}\square + R^{3+}$, results in increased "puckering" (inward rotation of the tetrahedra of the six-membered ring) and in a marked compression of the smaller 18c octahedra with which the larger 9b octahedra share edges. The volume of the unit cell is highly correlated ($r = 0.98$) to the weighted-mean size, $[9b–O + 4(18c–O)]/5$, of the 9b and 18c octahedra, which explains why lattice parameters can be successfully used to estimate octahedral-site occupancies. The chemistries of natural as well as synthetic tourmalines in the systems Na_2O-Al_2O_3-SiO_2-B_2O_3-H_2O and MgO-Al_2O_3-SiO_2-B_2O_3-H_2O are also rationalized on the basis of the observed structural trends.

INTRODUCTION

Surveys of the compositions of natural tourmalines by Foit and Rosenberg (1974, 1975, 1977) revealed the presence of coupled substitutions resulting in proton- and alkali-deficient tourmaline stoichiometries. THe dehydroxylation-type substitution, $(OH)^- + R^{2+} = O^{2-} + R^{3+}$, and alkali defect-type substitution, $R^+ + R^{2+} = {}^{3a}\square + R^{3+}$, produce intermediates between end-member schorl-dravite (other end-members as well) and a new series within the tourmaline group, $R^+_{1-x}R^{3+}_3R^{3+}_6 (BO_3)_3 Si_6O_{18}O_{3-x}(OH)_{1+x}$, defined by proton-deficient, $R^+R^{3+}_3R^{3+}_6 (BO_3)_3 Si_6O_{18}O_3(OH)$, and alkali cation-free, $\square R^{3+}_3R^{3+}_6 (BO_3)_3 Si_6O_{18}O_2(OH)_2$, end-members.

Tourmaline (olenite) with a composition closely approaching this series has been recently reported by Sokolov et al. (1986). Since the principle R^{3+} substituent is Al, our search for the alkali-deficient end-member has focused on deposits where tourmaline coexists with Al-rich minerals. Schorls from two tourmaline-dumortierite deposits, Jack Creek near Basin, Montana, and Ben Lomond, Hervey Range, North Queensland, Australia, have compositions closely approaching the alkali-free end-member (Foit, unpub. data).

In this paper the refined structural data on a alkali-deficient schorl from the Jack Creek deposit are integrated with the wealth of tourmaline structural information in the literature to provide a better understanding of the structural accommodation of these diverse substitutions.

ALKALI-DEFICIENT SCHORL

Crystal description and chemistry

A large number of tourmaline fragments were separated, using heavy liquids, from a ground hand specimen (JC-3) of grayish-green volcanic tuff consisting of 80% tourmaline in a matrix of fine-grained plagioclase feldspar, partially altered to sericite. Only one crystal out of several thousand examined was of sufficient size and optical uniformity to be used for X-ray data collection. An electron-microprobe anlaysis of the 0.05×0.10 mm crystal is given in Table 1. Despite the great amount of care taken to select an optically uniform crystal, there are significant variations in Fe, Mg, and Al across it, as reflected in the standard deviations of the analyses for these elements.

The formula in Table 1 is calculated on the basis of 31(O,OH,F) assuming that all of the Fe is divalent and that B_2O_3 and H_2O are present in stoichiometric amounts. Cation site assignments were made assuming that the Si deficiency in the tetrahedral ring is compensated for by

Al, the smaller 18c octahedral site is occupied exclusively by Al, and the remaining cations with the exception of Na occupy the larger 9b octahedral site. Although increasing the proportion of Fe^{3+} would improve the analytical total (i.e., increase it above 98.89 wt%), it would also increase the octahedral-site vacancy. Least-squares refinement of site multiplicities and bond-valence analysis (see Discussion) support these cation-site assignments.

Unit-cell and intensity-data collection

Intensity data were collected using a Nicolet R3M automated four-circle diffractometer and grahite-monochromatized MoKα radiation. X-ray photographs and the single-crystal intensity data confirmed the space group $R3m$. All X-ray reflections were sharp; no weak or diffuse "extra" reflections were observed. The unit-cell parameters, $a = 15.963(3)$ and $c = 7.148(2)$ Å ($V = 1577.3(6)$ Å^3) were obtained by least-squares refinement of 25 reflections in the 2θ range 24–40°.

A total of 3084 reflection intensities were collected in the $a_1^* a_2^* \pm c^*$ wedge over the range $2\theta = 5$–90° employing a θ-2θ scan with a range of 2° and a scan speed of 2.0–29.3°/min. Three standard reflections were measured every 100 reflections. The data were corrected for Lorentz and polarization effects and absorption ($\mu = 20.56$ cm^{-1}) using azimuthal scans.

Refinement

The refinement and crystallographic calculations were carried out using the SHELXTL crystallographic package (Revision 4.1; Sheldrick, 1984) and the 2678 unique structure factors for which $F_{obs} > 3\sigma(F_{obs})$. The trial positional parameters were those of V-bearing dravite (Foit and Rosenberg, 1979). Neutral-atom scattering factors and anomalous dispersion factors (Vol. 4, *International Tables for X-ray Crystallography*) and structure-factor weighting were used throughout the refinement.

The weighted residual (R_w) converged to a value of 0.070 after 5 cycles of refinement during which the scale factor, atom coordinates, and isotropic temperature factors were varied. The high residual suggested that the indexing of the data set was incompatible with the conventional orientation of the noncentrosymmetric structure (Foit and Rosenberg, 1979). Transformation ($hkl \rightarrow kh\bar{l}$) of the dataset indices and subsequent refinement reduced R_w to 0.055 with reasonable isotropic temperature factors for all atoms.

In the trial structure, the alkali site (3a) and octahedral site (9b) occupancies were defined by apportioning cation multiplicities on the basis of the microprobe data and structural formula given in Table 1. Refinement of the isotropic temperature factors and the atom multiplicities of these sites resulted in an insignificant lowering of R_w and only slight changes in the multiplicities, confirming the correctness of the original site assignments.

The H atom was then added to the model, and the refinement was completed with several cycles of least squares during which the positional and anisotropic ther-

TABLE 1. Electron-microprobe analysis of alkali-deficient schorl

Oxide	Wt%	Cations per 31(O,OH,F)
Na$_2$O	1.68(0.19)	0.55
CaO	0.01(0.02)	—
K$_2$O	0.02(0.01)	—
FeO	12.36(2.09)	1.75
MgO	1.29(1.45)	0.33
MnO	0.03(0.04)	—
Al$_2$O$_3$	35.02(1.73)	6.98
TiO$_2$	0.14(0.05)	0.02
SiO$_2$	34.42(0.94)	5.82
B$_2$O$_3$	10.30	3.00
F	0.27(0.12)	0.14
P	tr.	—
	95.54	
Less O ≡ F	−0.11	
	95.43	
H$_2$O	3.42	
	98.85	

Formula on the basis of 31(O,OH,F):
(Na$_{0.55}\square_{0.45}$)(Fe$_{1.75}$Al$_{0.80}$Mg$_{0.33}$Ti$_{0.02}\square_{0.10}$)Al$_6$(BO$_3$)$_3$(Si$_{5.82}$Al$_{0.18}$)O$_{18}$((OH)$_{3.86}$F$_{0.14}$)

Note: Standard deviations of 39 point analyses given in parentheses. Calculated density = 3.175 g/cm^3.

mal parameters (except for H, which was varied isotropically) and scale factor were varied. The final residuals are $R = \Sigma\|F\|_o - |F|_c|/|F|_o = 0.0428$, $R_w = [\Sigma w(|F|_o - |F|_c)^2/\Sigma w|F|_o^2]^{1/2} = 0.0369$ and $w = 1/(\sigma^2(F) + |g|F^2)$, where $g = 0.00026$, for the 2678 data used in the refinement and $R = 0.0538$ for the 3084 data collected (Table 2[1]).

The positional and thermal parameters and the interatomic distances and angles (uncorrected for thermal motion) are listed in Tables 3 and 4, respectively.

DISCUSSION

Structure of alkali-deficient schorl and tourmaline-group structural trends

The 13 refined tourmaline structures in the literature (Table 5) provide a wealth of structural data that can be used to examine the effects of chemical substitution on the configuration of the structure. Although the structures of these tourmalines are similar (Fig. 1a), the substitutions produce systematic changes in the principal structural units, some of which have been described by Foit and Rosenberg (1979) and Gorskaya and Frank-Kamenetskaya (1983). With the advent of a great deal more structural data, especially on tourmalines approaching the compositions of the ideal alkali- and proton-deficient end-members (Foit and Rosenberg, 1977), it is now possible to better define these effects, hereby providing a better understanding of the structure's remarkable tolerance to the diverse chemical substitution observed in nature and in the laboratory.

Alkali cation site and tetrahedral ring. The 9-coordinated 3a alkali cation site is formed by the six bridging
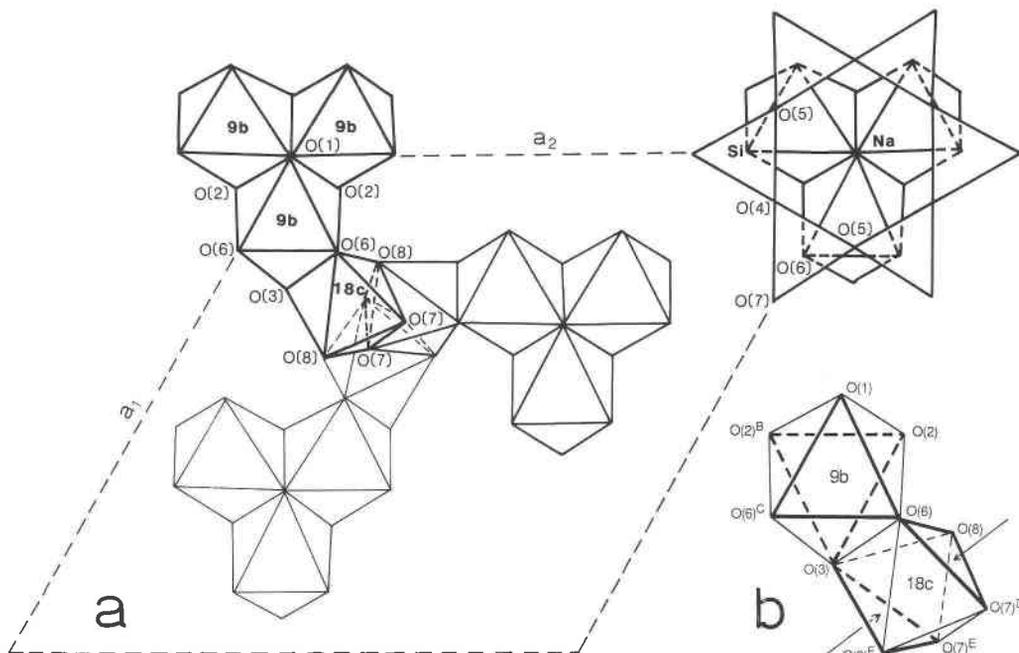
Fig. 1. (a) The tetrahedral and octahedral portions of the tourmaline structure projected down [001] (after Barton, 1969). (b) Details of the 9b and 18c octahedral portion of the structure. Bold lines and arrows define the bases of the octahedra and the axis of 18c compression, respectively. Superscripts on oxygen atoms indicate symmetry transformations in Table 4.

oxygens, O(4) and O(5), of the base of the tetrahedral ring and three oxygens, O(2), of the triad of edge-sharing 9b octahedra (Fig. 1a). The 3a cation site links the vertex-sharing 9b octahedral and tetrahedral ring clusters in the c-axis direction and is capable of adjusting its size and configuration within restricted limits to variations in cation occupancy (Foit and Rosenberg, 1979). There is a high linear correlation ($r = 0.83$) between Na + vacancy and the mean 3a–O bond distance; the alkali site is the largest when it is either vacant and/or occupied by Na (Fig. 2a).

The presence of smaller cations, principally Ca, reduces the size of the 3a site; the reduction is mainly accomplished through shortening of the 3a–O(4) and 3a–O(5) distances, resulting in changes in the configuration of the ring [ditrigonality (Barton, 1969) and crimping (Gorskaya et al., 1982)] or its component tetrahedra (distortion).

The distortion of the Si tetrahedra composing the ring as reflected in O–T–O angle variances [$(\sigma^2_{\theta(\text{tet})})$; Robinson et al., 1971] is highly correlated ($r = -0.85$) to the size of the 3a site (Fig. 2b). The Ca-rich tourmalines in Table

TABLE 3. Positional and thermal parameters ($\text{Å} \times 10^4$) for alkali-deficient schorl

Atom	Position	x	y	z	K*	U_{eq}	U_{11}	U_{22}	U_{33}	U_{23}	U_{13}	U_{12}
Na	3a	0	0	0.2215(7)	0.090(4)	247(13)	268(15)	U_{11}	207(23)	0	0	$U_{11}/2$
Fe**	9b	0.12292(4)	x/2	0.6297(1)	0.317(5)	77(4)	73(5)	44(3)	125(8)	$U_{13}/2$	−39(6)	$U_{11}/2$
Al**	9b	0.12292(4)	x/2	0.6297(1)	0.138(5)	186(32)	240(48)	237(34)	83(44)	$U_{13}/2$	36(37)	$U_{11}/2$
Al	18c	0.29800(4)	0.26134(4)	0.6094(1)	1	51(2)	49(2)	56(2)	47(2)	7(2)	−2(2)	26(2)
B	9b	0.1101(1)	2x	0.4535(4)	½	81(7)	72(7)	93(10)	85(9)	−0(8)	$U_{23}/2$	$U_{22}/2$
Si,Al	18c	0.19180(3)	0.18981(4)	0	1	58(1)	55(2)	56(2)	60(2)	−6(1)	−2(2)	26(1)
O(1)	3a	0	0	0.7771(7)	⅙	262(12)	339(16)	U_{11}	107(17)	0	0	$U_{11}/2$
O(2)	9b	0.06166(8)	2x	0.4871(3)	½	149(6)	217(8)	86(6)	101(8)	7(6)	$U_{23}/2$	$U_{22}/2$
O(3)	9b	0.2666(2)	x/2	0.5083(3)	½	127(6)	222(10)	1199(5)	74(7)	$U_{13}/2$	7(7)	$U_{11}/2$
O(4)	9b	0.09380(8)	2x	0.0694(3)	½	106(5)	81(5)	159(9)	104(7)	−6(7)	$U_{23}/2$	$U_{22}/2$
O(5)	9b	0.1877(2)	x/2	0.0922(3)	½	108(5)	153(9)	87(5)	105(7)	$U_{13}/2$	10(6)	$U_{11}/2$
O(6)	18c	0.1971(1)	0.1867(1)	0.7754(2)	1	89(4)	106(5)	105(5)	53(4)	−6(4)	−2(4)	49(4)
O(7)	18c	0.2854(1)	0.28601(9)	0.0783(2)	1	84(4)	79(5)	72(5)	81(5)	−11(4)	3(4)	22(4)
O(8)	18c	0.2099(1)	0.2706(1)	0.4397(2)	1	96(4)	68(5)	116(5)	107(5)	20(4)	8(4)	48(4)
H	9b	0.268(4)	x/2	0.398(8)	½	466(177)						

Note: Temperature factors of the form $\exp[-2\pi^2(h^2a^{*2}U_{11} + k^2b^{*2}U_{22} + \ldots + 2hka^*b^*U_{11}]$. Esd's are in parentheses.

* K = occupancy.

** Cations occupying the same site.

5 (liddicoatite, uvite, and dravite) have the smallest 3a sites and the most distorted tetrahedra, and the Jack Creek alkali-deficient schorl, which contains no Ca, has by far the largest 3a site and lowest tetrahedral distortion of any tourmaline examined to date (Fig. 2b). Most of the increased distortion results from a decrease in the O(4)–T–O(5) angle from 105.7° in aluminous dravite (AD2) to 101.2° in Ca-rich uvite because of a shortening of the O(4)–O(5) shared edge in response to greater 3a and T-site cation repulsion as well as lengthening of the T–O(4) bond because of increased valence saturation of O(4). The large size of the 3a site in alkali-deficient schorl relative to that in Cr-bearing dravite, schorl, tsilaisite, and buergerite—all of which contain appreciably more Na (Table 5)—may be due in part to the relaxation of oxygen atoms surrounding the partially vacant 3a site toward their bonded cation neighbors in the 9b octahedral, tetrahedral, and B sites (Shannon, 1976). This relaxation is most evident in the B and tetrahedral sites where there is very little substitution of other cations; the B–O(2) and T–O(5) distances in alkali-deficient schorl (Table 4) are shorter than those in Cr-bearing dravite, schorl, tsilaisite, and buergerite.

Although not apparent in Figure 1a, the six-membered tetrahedral ring deviates slightly from hexagonal symmetry, two related measures of which are the ring's crimping and ditrigonality. The bases of the tetrahedra are not parallel to (001) but are "crimped," alternately tilted up and down by a small amount. The degree of "crimping" is defined by Gorskaya et al. (1982) as $\Delta z = [zO_5 - (zO_4 + zO_7)/2] c$, where z is the coordinate of the oxygen atoms defining the base of the tetrahedron. Ditrigonality is defined by Barton (1969) as $\delta = (r_1 - r_s)/r_s$, where r_1 and r_s are the distances from O(4) and O(5), respectively, to the threefold axis (Barton, 1969). Ditrigonality is negatively correlated to crimping ($r = -0.79$); with increasing substitution of Ca in the 3a site and consequent shortening of the 3a–O(5) bond and O(4)–O(5) shared edge, the crimping of the ring decreases from 0.147 Å in Al-rich dravite (AD2) to 0.065 Å in buergerite (Fig. 2c), and the ditrigonality increases from 0 in tsilaisite to 0.038 in buergerite (Fig. 2d).

Studies of synthetic (Rosenberg and Foit, 1979, 1985; Rosenberg et al., 1986) and natural tourmalines (Foit and Rosenberg, 1977) have strongly suggested that $Al^{3+} \rightarrow Si$ substitution in the T_6O_{18} ring is both common and occasionally extensive. The positive correlation ($r = 0.70$) between [4]Al and the mean T–O distance in Figure 2e provides the first direct structural evidence. The scatter in the data is thought to reflect both analytical errors associated with Si determinations and the fact that frequently the structural formula giiven is based on an analysis of a sample from the type locality rather than an EMP analysis of the crystal used in the structure refinement. The limited amount of substitution of Al for Si in these natural tourmalines appears to only increase the size of the tetrahedra.

9b octahedral portion. In tourmalines the larger 9b octahedral site exhibits significantly more diverse and extensive substitutional chemistry than the smaller 18c octahedral site, as reflected in the wider range of mean bond distances involving 9b. With the substitution of smaller, more highly charged cations (i.e., Al), the 9b octahedron shrinks in size and becomes slightly more compressed in the c-axis direction. The compression ratio, which is the ratio of the mean length of the edges defining the sides to the mean length of the edges defining the bases (Table 4, Fig. 1b), decreases from 0.904 in schorl to 0.873 in buergerite.

Since the triads of edge-sharing 9b octahedra share polyhedral elements with other coordination groups in the

TABLE 4. Interatomic distances and angles of alkali-deficient schorl

Atoms	Distance (Å)	Atoms	Distance (Å)	Angles (°)
Si–O(4)	1.625(1)	O(4)–O(5)	2.599(2)	105.6(1)
Si–O(5)	1.639(1)	O(4)–O(7)	2.650(1)	109.8(1)
Si*–O(6)	1.610(1)	O(5)–O(7)	2.658(2)	109.5(1)
Si–O(7)	1.616(1)	Mean base edge	2.636	108.3
Mean	1.623	O(6)–O(4)*	2.676(2)	111.7(1)
		O(6)–O(5)*	2.669(2)	110.5(1)
		O(6)–O(7)	2.637(1)	109.7(1)
		Mean side edge	2.661	110.6
		Grand mean	2.648	
B–O(2)	1.360(4)	O(8)^A–O(2) 2×	2.383(2)	120.6(1)
B–O(8)^A 2×	1.383(2)	O(8)–O(8)^A	2.380(3)	118.7(2)
Mean	1.375	Mean	2.382	
Fe–O(1)	2.000(3)	O(1)–O(6)^C 2×	3.067(2)	99.2(1)
Fe–O(2)^B 2×	1.984(2)	O(2)–O(2)^B	2.953(2)	96.2(1)
Fe–O(3)	2.168(2)	O(3)–O(2)^B 2×	3.199(2)	100.7(1)
Fe–O(6)^C 2×	2.029(1)	O(6)–O(6)^C	2.813(3)	87.8(1)
Mean	2.032	Mean base edge	3.050	97.3
		O(1)–O(2)^B 2×	2.684(4)	84.7(1)
		O(1)–O(6) 2×	2.786(2)	87.9(1)
		O(3)–O(6)^B 2×	2.559(2)	75.1(1)
		Mean side edge	2.676	82.6
		Grand mean	2.863	
Al–O(3)	1.982(1)	O(3)–O(7)^F	2.852(2)	95.1(1)
Al–O(6)	1.871(1)	O(3)–O(8)^E	2.863(2)	95.4(1)
Al–O(7)^D	1.958(1)	O(6)–O(8)	2.706(2)	91.1(1)
Al–O(7)^E	1.880(1)	O(7)^D–O(6)	2.771(2)	92.7(1)
Al–O(8)	1.919(2)	O(7)^D–O(8)	2.882(2)	96.0(1)
Al–O(8)^E	1.889(2)	O(7)^E–O(8)^E	2.809(2)	96.4(1)
Mean	1.917	Mean base edge	2.814	94.5
		O(3)–O(6)	2.559(2)	83.2(1)
		O(3)–O(8)	2.802(2)	91.8(1)
		O(6)–O(8)^E	2.758(2)	94.4(1)
		O(7)^D–O(7)^E	2.722(1)	90.3(1)
		O(7)^D–O(8)^F	2.399(2)	77.1(1)
		O(7)^E–O(8)	2.399(2)	78.3(1)
		Mean side edge	2.607	85.9
		Grand mean	2.714	
Na–O(2)^B,F 3×	2.551(5)	O(2)^B–O(2)^B,F 3×	2.953(3)	70.7(1)
Na–O(4)^B,F 3×	2.812(3)	O(2)^B,F–O(4)^B,F 3×	3.115(3)	70.8(1)
Na–O(5)^B,F 3×	2.775(3)	O((2)^B,F–O(5)^B,F 6×	3.631(3)	86.3(1)
Mean	2.713	O(4)^B–O(4)^B,F 3×	4.492(2)	106.0(1)
		O(4)^B,F–O(5)^B,F 6×	2.599(2)	55.7(1)
		Mean	3.289	
H–O(3)	0.79(6)	O(3)–O(5)	3.168(3)	151.(2)
H–O(5)	2.45(6)			

Note: Standard deviation in parentheses. A: $y - x$, y, z. B: $y - x$, $-x$, z. C: x, $x - y$, z. D: $y - x + \frac{1}{3}$, $-x + \frac{2}{3}$, $z + \frac{2}{3}$. E: $-y + \frac{2}{3}$, $x - y + \frac{1}{3}$, $z + \frac{1}{3}$. F: $-y$, $x - y$, z. Transformations relate coordinates to those of Table 3.

* Positioned in adjacent unit cell.

TABLE 5. Least-squares refined tourmaline structures

Al-rich dravite (AD1) Schmetzer et al. (1979)
$(Na_{0.63}Ca_{0.27}\square_{0.08}K_{0.02})(Mg_{2.51}Al_{0.35}Ti_{0.06}\square_{0.05}V_{0.02}Fe_{0.01})Al_6(B_{2.80}Al_{0.20})(Si_{5.97}Al_{0.03})O_{27}O_{0.28}(OH)_{3.72}$

Al-rich dravite (AD2) Gorskaya et al. (1985)
$(Na_{0.47}Ca_{0.02}\square_{0.51})(Mg_{1.91}Al_{0.98}Fe_{0.07}Ti_{0.02}\square_{0.02})Al_6B_3(Si_{5.98}Al_{0.02}O_{18})O_{27}O_{0.61}(OH)_{3.39}$

Al-rich elbaite (AE) Gorskaya et al. (1982)
$(Na_{0.46}\square_{0.45}Ca_{0.08}K_{0.01})(Al_{2.18}Li_{0.53}Mn_{0.22}\square_{0.04}Fe_{0.02}Ti_{0.01})Al_6B_{2.96}Si_{6.09}O_{27}O_{1.47}(OH)_{2.44}F_{0.09}$

Buergerite (B) Barton (1969)
$(N_{0.83}Ca_{0.13}K_{0.02}\square_{0.02})(Fe^{3+}_{1.81}Al_{0.88}Fe^{2+}_{0.19}Ti_{0.06}Mg_{0.03}Mn_{0.02}\square_{0.01})(Al_{5.44}Fe_{0.50}Mg_{0.01}Ti_{0.01})B_3(Si_{5.73}B_{0.27})O_{27}O_{2.51}F_{1.03}(OH)_{0.46}$

Cr-bearing dravite* (CD) Nuber and Schmetzer (1979)
$(Na_{0.84}Ca_{0.16}K_{0.02})(Mg_{2.46}Cr_{1.14}Fe^{2+}_{0.14}Mn_{0.02}Ti_{0.01})(Al_{4.43}Cr_{1.33}Fe^{3+}_{0.24})B_{2.91}(Si_{5.77}Al_{0.23})O_{27}O_{2.4}(OH)_{1.6}$

Dravite (D) Buerger et al. (1962)
$(Ca_{0.60}Na_{0.39}K_{0.01})Mg_3(Al_{5.42}Mg_{0.55}Fe^{2+}_{0.03})B_3(Si_{5.84}Al_{0.16})O_{27}O_{0.61}(OH)_3F_{0.49}$

Elbaite (E) Donnay and Barton (1972)
$(Na_{0.56}Mn_{0.15}Ca_{0.14}\square_{0.13}B_{0.02})(Al_{1.59}Li_{1.25}Mn_{0.13}Fe^{2+}_{0.03})Al_6B_3(Si_{5.98}B_{0.02})O_{27}O_{0.53}(OH)_{2.87}F_{0.60}$

Liddicoatite (L) Nuber and Schmetzer (1981)
$(Ca_{0.65}Na_{0.35})(Li_{1.40}Al_{1.60})Al_6B_3Si_6O_{27}(O,OH,F)_4$

Schorl (S) Fortier and Donnay (1975)
$(Na_{0.88}Ca_{0.11}K_{0.01})(Fe^{2+}_{1.64}Al_{0.44}Fe^{3+}_{0.42}\square_{0.16}Mg_{0.11}Ca_{0.07}Ti_{0.07}Li_{0.07}Mn_{0.02})(Al_{5.61}Fe_{0.39})B_3Si_6O_{27}O_{0.29}(F,OH)_{3.71}$

Tsilaisite (T) Nuber and Schmetzer (1984)
$(Na_{0.85}\square_{0.11}Ca_{0.04})(Al_{1.53}Mn_{0.93}Li_{0.42}\square_{0.12})Al_6B_3Si_6O_{27}O_{0.90}(OH,F)_{3.10}$

Uvite (U) Schmetzer et al. (1979)
$(Ca_{0.62}Na_{0.36}K_{0.01}Sr_{0.01})Mg_3(Al_{5.45}Mg_{0.44}Ti_{0.05}\square_{0.02}V_{0.02}Ca_{0.02})(B_{2.85}Al_{0.15})(Si_{5.99}Al_{0.01})O_{27}O_{0.27}(OH)_{3.29}F_{0.44}$

V-bearing Dravite (V) Foit and Rosenberg (1979)
$(Na_{0.44}Ca_{0.36}Mg_{0.18}K_{0.02})(Mg_{1.87}V_{0.76}Cr_{0.19}Fe^{2+}_{0.18})(Al_{5.56}V_{0.38}Ti_{0.06})(Si_{5.63}Al_{0.37})(B_{2.98}\square_{0.02})O_{27}O_{1.10}(OH)_{2.58}F_{0.32}$

* Structural formula generated from chemical data given by the authors yields a significant excess of cations.

TABLE 6. Bond valences of alkali deficient schorl

Anion	3a	9b	18c	B	Si	ΣC^v	Occupancy	ΔV
O(1)		0.412 (3)				1.236	OH⁻, F⁻	+0.236
O(2)	0.091 (1)	0.427 (2)		1.031 (1)		1.976	O²⁻	−0.024
O(3)		0.270 (1)	0.405 (2)			1.080	OH⁻, F⁻	+0.080
O(4)	0.047 (1)				0.989 (2)	2.025	O²⁻	+0.025
O(5)	0.052 (1)				0.962 (2)	1.976	O²⁻	−0.024
O(6)		0.387 (1)	0.573 (1)		1.019 (1)	1.979	O²⁻	−0.021
O(7)			0.558 (1) 0.440 (1)		1.006 (1)	2.004	O²⁻	+0.004
O(8)			0.543 (1) 0.497 (1)	0.984 (1)		2.024	O²⁻	+0.024
L(mean)	2.713	2.032	1.917	1.375	1.623			
L(max)	3.13	2.49	2.26	1.87	2.13			
p(exp)	6.506	4.437	5.589	2.777	3.176			
V(i)	0.55/9	2.30/3	3.00/6	3.00/3	3.97/4			

Note: Number of bonds received by anion in parentheses.

$\longrightarrow$

Fig. 2. Variations in structural parameters for 13 refined tourmaline structures. See Table 5 for tourmaline abbreviations (DS = alkali-deficient schorl) and the text for parameter definitions. At 99% confidence level, the critical value of $r = 0.68$ for a sample size of 13.
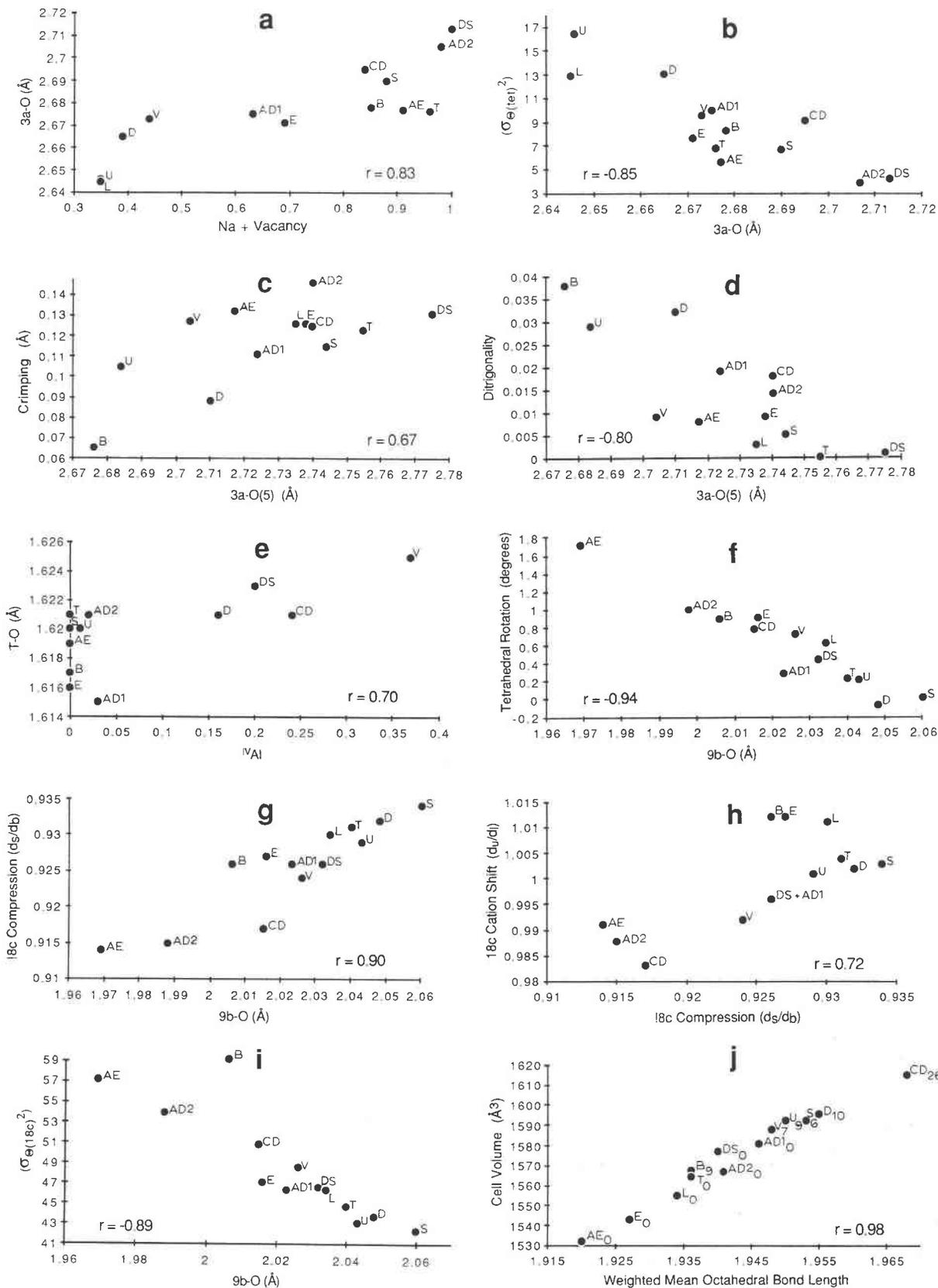
structure, variations in the size of the 9b site have systematic effects on the configurations of these groups, some of which have been described earlier by Foit and Rosenberg (1979) and Gorskaya and Frank-Kamenetskaya (1983). Each 9b octahedron shares the O(6) apical oxygens of two adjacent tetrahedra of the six-membered ring (Fig. 1a); with a decrease in its size, O(6) is displaced toward the threefold axis producing a puckering of the ring. The individual tetrahedra rotate about the O(4)–O(5) edge and elongate in the direction of the c axis (Fig. 1a). The angle of rotation, which is measured from (001) to the normal to O(4)–O(5) from O(7), is highly correlated to 9b–O ($r = -0.94$) and ranges from approximately 0° in dravite to 1.71° in Al-rich elbaite (Fig. 2f). The amount of elongation, which is the ratio of the mean length of the edges defining the sides of the tetrahedron to the mean length of those defining the base (Table 4, Fig. 1b), ranges from 1.007 in uvite to 1.016 in Al-rich elbaite and is weakly correlated ($r = -0.55$) to mean 9b–O distance. Thus, in Al-rich tourmalines like Al-rich elbaite where 73% of the 9b octahedral sites is occupied by Al, the tetrahedral ring is significantly puckered with individual tetrahedra rotated and elongated toward the c axis.

Although the preceding analysis suggests that cation substitution in the 3a site primarily affects the crimping and ditrigonality of the ring and the distortion of the tetrahedra whereas substitution in 9b mainly affects the puckering of the ring, the effects are not mutually exclusive and are likely responsible for much of the expected scatter in the data in Figures 2a–2f. This is because the tetrahedral ring shares polyhedral elements (albeit fewer) with the 9b and 18c octahedral sites as well as with the 3a alkali site.

18c octahedral portion. Each of the small 18c octahedra shares three edges with adjacent octahedra: two, O(7)^F–O(8) and O(7)^D–O(8)^E, with adjacent 18c octahedra to form a helix about the 3_1 screw axis and one, O(3)–O(6), with a 9b octahedron (Fig. 1a). Inasmuch as these shared edges are appreciably shorter than the others, the 18c octahedra of all of the tourmalines examined are appreciably compressed with the axis of compression, unlike that of the 9b octahedra, lying approximately 70° from the c axis (arrows, Fig. 1b). Using the shared edges to define the sides of the 18c octahedron, this compression can be quantified in a manner similar to that for the 9b octahedron, as the ratio of the mean length of the edges defining the sides (d_s) to the mean length of the edges defining the bases (d_b) (Table 4).

The appreciable variation in the size of the 9b site (ranging from 1.969 Å in Al-rich elbaite to 2.060 Å in schorl) due to extensive cation substitution is highly correlated ($r = 0.90$) to 18c compression (Fig. 2g). Most of this compression is due a shortening of five [O(3)–O(6), O(3)–O(8), O(7)^D–O(7)^E, O(7)^F–O(8), O(7)^D–O(8)^E] of the six edges that define the sides of the octahedron (Fig. 1b, Table 4). The highest correlations are between the mean 9b–O distance and the O(3)–O(6), O(3)–O(8) and O(7)^D–O(7)^E edges, all of which have atoms shared with the 9b octahedron or the Si tetrahedron.

O(3)–O(6) is the shared edge between the 9b and 18c octahedra (Fig. 1b). The length of this edge and the O(3)–18c–O(6) angle are largely controlled by the size of the cation occupying the 9b site as evidenced by the strong linear correlations between mean 9b–O distance and these parameters ($r = 0.89$ and 0.79, respectively) and the weak correlations between mean 18c–O and these parameters ($r = 0.53$ and -0.33, respectively). The high correlations between mean 9b–O distance and O(3)–O(6) and O(3)–O(8) distances ($r = 0.89$ and 0.76, respectively) may be due in part to the dehydroxylation substitution, (OH)$^-$ + R^{2+} = O^{2-} + R^{3+}. The substitution of R^{3+} cations for R^{2+} cations, which compensates for the loss of protons from O(1) and O(3), is thought (Foit and Rosenberg, 1977) to take place largely in the 9b octahedral site. If this is the case, variations in the length of shared edges involving O(3) in response to changes in the H coordination of O(3) would be expected to be related to the size of the 9b site.

Compression of the 18c site due to substitution of smaller, more highly charged cations in the 9b site is accompanied by an apparent shift [d_u/d_l, where $d_u = $ (18c–O(7)^D + 18c–O(7)^E)/2 and $d_l = $ (18c–O(3) + 18c–O(6))/2] of the 18c cation away from the O(3)–O(6) shared edge toward the O(7)^D–O(7)^E edge (Figs. 1b, 2h). Although the cation shift must be partly due to increased octahedral-cation repulsion across the O(3)–O(6) edge, it also appears to be the product of movement of the O(7) atom, which is shared between the 18c octahedron and the Si tetrahedron (Fig. 1a). The smaller the 9b site the more "puckered" the tetrahedral ring and the more O(7) is rotated toward the 18c site shortening the 18c–O(7)^D bond and making the 18c octahedron smaller and more compressed. This is why, of all the 18c–O bonds, 18c–O(7)^D is the most weakly correlated to mean 18c–O distance (18c cation occupancy) and most strongly correlated to mean 9b–O distance.

O(7)^E–O(8) and O(7)^D–O(8)^E are the symmetry-equivalent edges shared by each 18c octahedron forming the helix around the 3_1 screw axis (Fig. 1a). The length of these symmetry-equivalent edges and the O(7)^D–18c–O(8)^E angle are highly correlated to the mean 18c–O distances, $r = 0.93$ and 0.83, respectively. The O(7)^D–18c–O(8)^E and O(7)^D–18c–O(7)^E angles are the only ones in the 18c octahedron highly correlated ($r = 0.83$ and 0.83, respectively) to mean 18c–O distance, which is consistent with the observation that substitution in the 18c site has little or no effect on overall distortion of the 18c octahedron ($\sigma^2_{\theta(18c)}$). Thus, although the size of the 18c octahedron and two central angles are largely controlled by the size of the 18c cation, the overall distortion of the 18c octahedron appears to be primarily influenced by the size of the 9b cation (Fig. 2i).

Unit-cell volume variations are a linear function of the dimensions of the 9b and especially the 18c octahedra; the greater the mean 9b–O and 18c–O bond lengths, the greater the cell volume (Fig. 2j). The 0.98 correlation coefficient indicates that 96% of the observed variability in unit-cell volume is due to a linear dependence on the

weighted-mean octahedral bond lengths, [9b–O + 4(18c–O)]/5. A linear dependence of 76% ($r = 0.87$) between 18c–O bond length and volume strongly suggests that the cation occupancy of the smaller 18c octahedral site is the main contributor to changes in cell volume. The greater influence of the 18c octahedra on cell volume is likely due to their greater number in the unit cell (twice as many 18c as 9b octahedra) and their function. Helices of edge-sharing 18c octahedra parallel to the c axis link the more rigid 9b octahedral and tetrahedral ring clusters to form the tourmaline structure (Fig. 1a). Any increase in the size of 18c due to partial substitution of cations larger than Al^{3+} (Fe^{3+}, Mg, Cr^{3+}, V^{3+}), therefore, would have a major effect on cell volume. Examination of the site occupancies of the 13 refined tourmaline structures (Table 5; Fig. 2j, subscripts indicate the percentage occupancy of the 18c site by cations other than Al^{3+}) reveals that tourmalines with Mg, Cr, Fe, and V in the 18c site generally have the largest cell volumes. The slightly smaller than expected unit cell of buergerite probably results from the shrinkage of 9b due to a 90% occupancy by Al and Fe^{3+} more than compensating for the expansion of the 18c site due to the presence of 8% Fe^{3+}. The strong coupling between cell volume and octahedral-site occupancy explains why cell parameters often can be successfully employed to estimate site occupancy in tourmalines with simple stoichiometries (Rosenberg and Foit, 1985).

The limited substitution of cations larger than Al in the 18c site might be necessary in some tourmalines to compensate structurally for extensive substitution of large cations in 9b. Although mean 9b–O and mean 18c–O bond distances are not significantly correlated, the strong correlation between mean 9b–O and 18c compression (and angle variance) suggests that the sites must in some way influence each other's cation occupancy. One possible mechanism involves rotation of the tetrahedra that share O(7) with the 18c octahedra. The larger the 9b site, the less puckered the tetrahedral ring and the more O(7) is rotated away from the 18c site, in effect making it larger. This coupled with the need for a longer O(3)–O(6) shared edge between 9b and 18c may in effect make the 18c site larger and more receptive to larger cations. The chemical data in Table 5 in the literature suggest that tourmalines having an appreciable proportion of large cations (Fe, Mg) in 9b also have a small proportion of them in 18c.

Protons. The protons in the tourmaline structure are principally bound to the O(1) and O(3) atoms both of which constitute part of the 9b and 18c octahedral coordination spheres. As is the case in other tourmaline structure refinements (Gorskaya et al., 1982; Gorskaya and Frank-Kamenetskaya, 1983; Foit and Rosenberg, 1979; Tippe and Hamilton, 1971), only the positional parameters of the proton bound to O(3) in the alkali-deficient schorl could be successfully refined because of its higher multiplicity. The hydrogen-bond geometry—H–O(3) = 0.79(6) Å, H–O(5) = 2.45(6) Å, and O(3)–H···O(5) = 151(2)°—is similar to that observed in other refined tourmaline structures.

Since information regarding the proton-site occupancies could not be obtained directly from X-ray studies, the proton occupancies of the alkali-deficient schorl were estimated based on the agreement between calculated and ideal anionic valence sums (Donnay and Allmann, 1970). The bond valence sums for O(1) and O(3) (1.236 and 1.080 v.u., respectively) in alkali-deficient schorl (Table 6), calculated assuming a stoichiometric amount of OH^{-} [12(OH,F) per unit cell], significantly exceed the expected value of 1.000 v.u. for an anion occupancy of (OH,F). This suggests, as was the case for V-bearing tourmaline (Foit and Rosenberg, 1979), that there is significantly less than an ideally stoichiometric amount of (OH + F) in the structure. Adjustment of the anion occupancies of O(1) and O(3) consistent with the observed calculated valence sums, Σc^{v}, yields $O_{0.24}(OH,F)_{0.76}$ and $O_{0.08}(OH,F)_{0.92}$, respectively. The structural formula of the alkali-deficient schorl, assuming this (OH) stoichiometry, is $(Na_{0.55}\square_{0.45})$-$(Fe^{2+}_{1.76}Al_{0.89}Mg_{0.33}Ti_{0.02})Al_6(BO_3)_3(Si_{5.86}Al_{0.14})O_{18.48}(OH_{3.38}$-$F_{0.14})$. It is noteworthy that this formula lacks the small 9b octahedral vacancy present in the formula based on ideal OH stoichiometry (Table 1).

Implications. The foregoing data have important implications regarding substitutional chemistry of natural and synthetic tourmalines. As shown in Figure 2b, the Jack Creek alkali-deficient schorl with an alkali-site occupancy of $Na_{0.55}\square_{0.45}$ has the least distorted tetrahedra of any tourmaline structure examined to date, and substitutions of cations smaller than Na (principally Ca) markedly distort the tetrahedra of the six-membered ring and increase its ditrigonality. Virtually all natural tourmalines, even the Ca-rich tourmalines uvite (Dunn et al., 1977b) and liddicoatite (Dunn et al., 1977a) contain appreciable Na and/or are alkali site deficient. Although tourmalines have been reported with nearly 100% occupancy of the 3a site by Ca (Bridge et al., 1977), the presence of Na and or a vacancy appears to mitigate the distortion produced by Ca substitution. This would also explain why tourmalines with an alkali-site vacancy grow so readily in the system MgO-Al_2O_3-SiO_2-B_2O_3-H_2O (Rosenberg and Foit, 1979, 1985; Werding and Schreyer, 1984). Assuming 100% occupancy of the nine-coordinated 3a site by Mg and a mean Mg–O bond distance of 2.34 Å (Shannon, 1976), an extrapolation of the data in Figure 2b, using the regression equation $\sigma^{2}_{\theta(\text{tet})} = 419.0 - 153.2(3a$–$O)$ yields a tetrahedral bond-angle variance of $(60.5°)^2$. This is three times the variance observed for the tetrahedra in uvite, the most distorted of the natural tourmalines, which suggests that if Mg is present in the 3a alkali site of tourmaline grown in alkali-free systems, it is likely to be accompanied by a significant vacancy. This is largely true of the tourmalines grown at 600–800 °C and 1 kbar by Rosenberg and Foit (1979, 1985). However, those grown in the temperature range 400–450 °C at 1 kbar by Rosenberg and Foit (1979, 1985) were shown, on the basis of cell-parameter variations, to have 90–100% Mg occupancy of the 3a site, which contradicts the claim of Werding and Schreyer (1984) that tourmalines grown in this system over the temperature

and pressure ranges 300–870 °C and 1–20 kbar, respectively, have an invariant composition corresponding to the ideal alkali-deficient end-member, $\square(Mg_2Al)Al_6(BO_3)_3(Si_6O_{18})(OH)_4$.

Although variable amounts of Mg have been reported in the 3a site of natural tourmalines, most notably 18% in V-bearing dravite (Foit and Rosenberg, 1979) and 50% in "magnodravite" Wang and Hsu (1966), Mg occupancies approaching 100% do seem crystal-chemically unreasonable. The formulas of the alkali-free tourmalines were calculated assuming that the 18c site is occupied solely by Al (Rosenberg and Foit, 1979, 1985). Given the much greater influence of the size of the 18c site over that of the 9b site on cell volume, partial occupancy of the 18c site by Mg would probably lead to incorrect site-occupancy calculations. The fact that the alkali-free tourmalines synthesized at 400–450 °C have the smallest lattice parameters, almost identical to those of elbaite and smaller than even those of tourmalines synthesized in the system Na_2O-Al_2O_3-SiO_2-B_2O_3-H_2O (Rosenberg et al., 1986), validates the assumption that the 18c site is fully occupied by Al. It is likely, therefore, that the 3a sites of tourmalines synthesized in the temperature range 400–450 °C by Rosenberg and Foit (1979, 1985) are fully occupied by Mg but that these tourmalines are metastable.

Calculation of the tetrahedral-angle variance assuming 100% occupancy of the 3a site by K and a mean K–O bond distance of 2.92 Å (Shannon, 1976) yields a tetrahedral-angle variance of $(28.3°)^2$. Although the nature of the tetrahedral distortion produced by substitution of a cation as large as K in the 3a site is not clear, the magnitude of the calculated angle variance suggests that the substitution would not be extensive, a conclusion supported by the low concentration of K found in natural samples. Taylor and Terrell (1967), however, reported synthesizing a tourmaline with 100% occupancy of the 3a site by K in hydrothermal experiments over the temperature range 417–490 °C. This tourmaline, like those in which the 3a site is fully occupied by Mg, is probably metastable.

Tourmaline approaching the proton-deficient and alkali-cation–deficient series $R^+_{1-x}R^{3+}_3R^{3+}_6(BO_3)_3Si_6O_{18}O_{3-x}(OH)_{1+x}$ has been found in nature (olenite, $(Na_{0.51}K_{0.01}Ca_{0.05}\square_{0.43})(Al_{2.91}Mn_{0.07}Fe_{0.02}Ti_{0.01})Al_6(BO_3)_3Si_6O_{20.53}(OH_{1.44}F_{0.03})$; Sokolov et al., 1986) and somewhat more aluminous and proton-enriched tourmalines have been synthesized in the system Na_2O-Al_2O_3-SiO_2-B_2O_3-H_2O by Rosenberg et al. (1986). In the synthetic tourmalines, the most aluminous of which has the formula $(\square_{0.06}Na_{0.94})Al_3Al_6(BO_3)_3(Si_{4.22}Al_{1.78})O_{19.2}(OH)_{2.80}$, both the 9b and 18c octahedral sites and a significant proportion of the tetrahedral sites are occupied by Al. The closest natural analogue for which detailed structural data are available is Al-rich elbaite (Gorskaya et al., 1982; Table 5) in which 73% of the 9b octahedral and none of the tetrahedral sites are occupied by Al. Since occupancy of the octahedral sites, especially 18c, strongly influences cell volume, it might be expected that the synthetic Na-Al tourmalines would have the smallest cell volumes. Surprisingly, the cell volume reported by Rosenberg et al. (1986) for a Na-Al tourmaline is 1552.57 Å³, which is considerably larger than that of Al-rich elbaite (1532.32 Å³), elbaite (1543.0 Å³), or olenite (1533.7 Å³). Apparently, the unit-cell expansion produced by significant Al → Si substitution partially offsets the contraction due to increased substitution of Al in the 9b site; a weak linear correlation ($r = 0.55$) between cell volume and [4]Al was observed for the tourmalines listed in Table 5. No significant correlation between mean T–O distance and either crimping or ditrigonality was observed in the natural tourmalines (Table 5), probably because a maximum of only 6% of the tetrahedral sites in these tourmalines is occupied by Al. The extensive substitution of [4]Al in these synthetic tourmalines, as much as 30%, must result in a significant increase in the O(4)–O(5) tetrahedral edge and increased crimping of the ring. Since these changes favor occupancy of the 3a site by a large cation like Na (Fig. 2c) and a significant vacancy would result in additional valence undersaturation of O(4) and O(5) (Table 6), extensive substitution of Al in the tetrahedral site is likely coupled to nearly full occupancy of the 3a site. Indeed, synthetic Na-Al tourmalines with the most [4]Al tend to have the highest 3a-site occupancy (Rosenberg et al., 1986), and in schorls from the Ben Lomond uranium-molybdenum-zinc deposit, North Queensland, Australia (Foit, unpub. data), [4]Al substitution is charge-balanced by (Na,Ca) substitution for a vacancy (or Ca for Na) in the 3a site.

Although extensive concomitant substitution of Al in both the ring and the triad of edge-sharing 9b octahedra would seemingly result in a mismatch of these vertex-sharing components, the structure is clearly capable of accommodating it. Part of the reason lies in the fact that Al substitution in 9b affects the ring in a geometrically different and largely independent way from tetrahedral Al substitution. Occupancy of the 9b site by a small cation like Al elongates the tetrahedra and increases the "puckering" of the tetrahedral ring whereas increased [4]Al substitution probably increases the ring "crimp." The full occupancy of 9b by Al in the synthetic tourmalines should also result in slightly greater compression of the 18c site (Fig. 2g) than is observed in Al-rich elbaite.

Tourmaline crystals grow quite readily in the system Na_2O-Al_2O_3-SiO_2-B_2O_3-H_2O, and attempts are now being made to grow them large enough for single-crystal studies. Crystal-structure refinements of a carefully selected synthetic tourmaline and olenite would test many of the ideas presented in this paper.

REFERENCES CITED

Barton, R., Jr. (1969) Refinement of the crystal structure of buergerite and the absolute orientation of tourmalines. Acta Crystallographica, B25, 1524–1533.

Bridge, P.J., Daniels, J.L., and Pryce, M.S. (1977) The dravite crystal bonanza of Yinnietharra, Western Australia. Mineralogical Record, 8, 109–110.

Buerger, M.J., Burnham, C.W., and Peacor, D.R. (1962) Assessment of several structures proposed for tourmaline. Acta Crystallographica, 15, 583–590.

Donnay, G., and Allmann, R. (1970) How to recognize O^{2-}, $(OH)^-$, and H_2O in crystal structures determined by X-rays. American Mineralogist, 55, 1003–1015.

Donnay, G., and Barton, R., Jr. (1972) Refinement of the crystal structure of elbaite and the mechanism of tourmaline solid solution. Tschermaks Mineralogische und Petrographische Mitteilungen, 18, 273–286.

Dunn, P.J., Appleman, D.E., and Nelen, J.E. (1977a) Liddicoatite, a new calcium end-member of the tourmaline group. American Mineralogist, 62, 1121–1124.

Dunn, P.J., Appleman, D.E., Nelen, J.E., and Norberg, J. (1977b) Uvite, a new (old) common member of the tourmaline group and its implications for collectors. Mineralogical Record, 8, 100–108.

Foit, F.F., Jr., and Rosenberg, P.E. (1974) Coupled substitutions in tourmaline (abs.). EOS, 55, 467.

——— (1975) Aluminobuergerite, $Na_{1-x}Al_3Al_6B_3Si_6O_{27}O_{3-x}(OH)_{1+x}$, a new end-member of the tourmaline group. EOS. 56, 461.

——— (1977) Coupled substitutions in the tourmaline group. Contributions to Mineralogy and Petrology, 62, 109–127.

——— (1979) The structure of vanadium-bearing tourmaline and its implications regarding tourmaline solid-solutions. American Mineralogist, 64, 788–798.

Fortier, S., and Donnay, G. (1975) Schorl refinement showing compositional dependence of the tourmaline structure. Canadian Mineralogist, 13, 173–177.

Gorskaya, M.G., and Frank-Kamenetskaya, O.V. (1983) Structural-crystal chemical features of tourmalines. In Yu. G. Papulov, Ed., Sovremennye Problemy Kristallokhimii Materialy Soveshchaniya-Seminara po Sovremennym Problemam i Metodike Prepodavaniya Kristallokhimii, 4th, Kalinin Gos University, Kalinin, USSR.

Gorskaya, M.G., Frank-Kamenetskaya, O.V., and Rozhdestvenskaya, I.V. (1982) Refinement of the structure of Al-rich elbaite and some aspects of the crystal chemistry of tourmalines. Soviet Physics. Crystallography, 27(1), 63–66.

Gorskaya, M.G., Frank-Kamenetskaya, O.V., Rozhdestvenskaya, I.V., Sokolov, P.B., and Frank-Kamenetskii, V.A. (1985) Crystal-structure of aluminum-rich dravite; structural-crystal chemical characteristics of magnesium-aluminum-tourmalines. Kristallokhimiya Strukturnyi Tipomorfizm Mineralov, 1985, 105–114.

International tables for X-ray crystallography. (1974) Volume IV. Kynoch Press, Birmingham, England.

Nuber, Bernhard, and Schmetzer, K. (1979) Die gitterposition des Cr^{3+} im tourmalin: Struktverfeinerung eines Cr-reichen Mg-Al tourmalins. Neues Jahrbuch für Mineralogie Abhandlungen, 137, 184–197.

——— (1981) Strukturverfeinerung von Liddicoatit. Neues Jahrbuch für Mineralogie Monatschefte, 215–219.

——— (1984) Structural refinement of tsilaisite (manganese tourmaline). Neues Jahrbuch für Mineralogie Monatschefte, 301–304.

Robinson, Keith, Gibbs, G.V., and Ribbe, P.H. (1971) Quadratic elongation: A quantitative measure of distortion in coordination polyhedra. Science, 172, 567–570.

Rosenberg, P.E., and Foit, F.F., Jr. (1979) Synthesis and characterization of alkali-free tourmaline. American Mineralogist, 64, 180–186.

——— (1985) Tourmaline solid solutions in the system $MgO-Al_2O_3-SiO_2-H_2O$. American Mineralogist, 70, 1217–1223.

Rosenberg, P.E., Foit, Jr., F.F., and Ekambaram, V. (1986) Synthesis and characterization of tourmaline in the system $Na_2O-Al_2O_3-SiO_2-B_2O_3-H_2O$. American Mineralogist, 71, 971–976.

Schmetzer, Karl, Nuber, B., and Abraham, K. (1979) Crystal chemistry of magnesium-rich tourmalines. Neues Jahrbuch für Mineralogie Abhandlungen, 136, 93–112.

Shannon, R.D. (1976) Revised effective ionic radii and systematic studies of interatomic distances in halides and chalcogenides. Acta Crystallographica, A32, 751–767.

Sheldrick, G.M. (1984) Shelxtl, a crystallographic computing package, Revision 4.1. Nicolet Analytical Instruments, Madison, Wisconsin.

Sokolov, P.B., Gorskaya, M.G., Gordienko, V.V., Petrova, M.G., Kretser, Yu.L., and Frank-Kamenetskii, V.A. (1986) Olenite, $Na_{1-x}Al_3Al_6B_3Si_6O_{27}$-$(O,OH)_4$—A new high-alumina mineral of the tourmaline group. Zapiski Vsesoyuznogo Mineralogicheskogo Obshchestva, 115, 119–123 (in Russian).

Taylor, A.M., and Terrell, B.C. (1967) Synthetic tourmalines containing elements of the first transition series. Journal of Crystal Growth, 1, 238–244.

Tippe, A., and Hamilton, W.C. (1971) A neutron diffraction study of the ferric tourmaline, buergerite. American Mineralogist, 516, 101–113.

Wang, S., and Hsu, X. (1966) A new variety of dravite and its significance in mineralogy. Kexu Tangbao, 17, 91–96.

Werding, G., and Schreyer, W. (1984) Alkali-free tourmaline in the system $MgO-Al_2O_3-SiO_2-B_2O_3-H_2O$. Geochimica et Cosmochimica Acta, 48, 1331–1344.